

Supplemental Tables and Figures

Supplemental Table 1. Primer sequences for real-time PCR

Gene	Forward (5' to 3')	Reverse (5' to 3')
human LBH	ctctgactatctgagatcggctgag	gcaggcggtccttcagtttg
human VEGFA	cagaatcatcacgaagtgggtg	gaagatgtccaccagggtc
human CRYAB	agagcacctgttgagctgatc	ggagaagtgccttcacatccaggt
human Vimentin	cgttccaagcctgacctcac	gcatccacttcgcaggtgag
human E-cadherin	cacctgattcttaggcagatgcca	gtggtcagggtcactggcatg
human GAPDH	ggcaaggatcatcccagagct	cccaggatgcccttagtggtg
human CD63	cagtggatcatcatcgagctg	atcgaagcagtggtggtgtt

GAPDH, glyceraldehyde-3-phosphate dehydrogenase; CRYAB, α B-Crystallin.

Supplemental Table 2. Antibodies for western blotting and Immunofluorescence

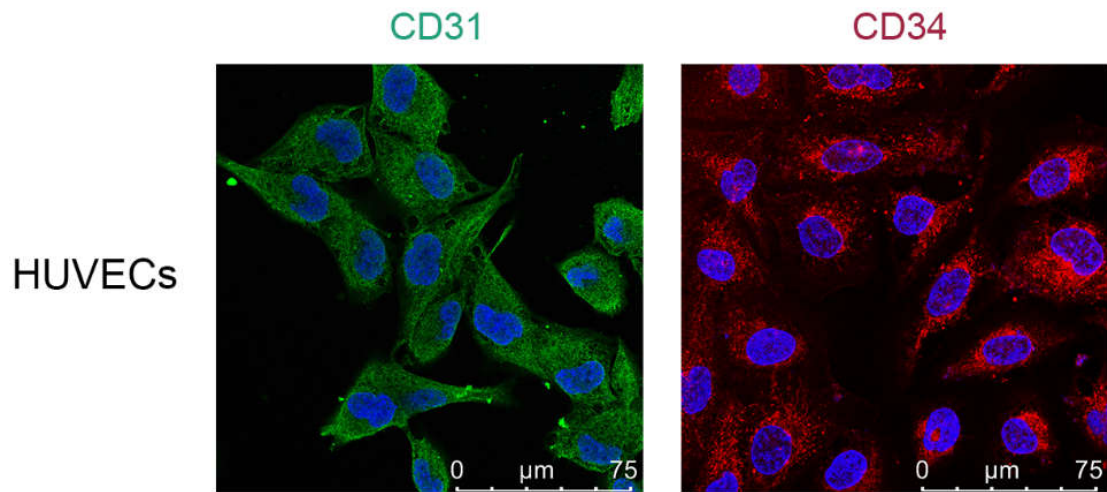
Antibodies	Product numbers	Applications
rabbit anti-LBH	Abcam, ab173737	WB (1:100)
rabbit anti-LBH	Abcam, ab122223	IF (1:100)
rabbit anti-CRYAB	Abcam, ab76467	WB (1:500)
rabbit anti-phospho-CRYAB	Abcam, ab5577	WB (1:2000); IF (1:100)
mouse anti-EEA1	Abcam, ab70521	IF (1:100)
mouse anti-Vimentin	Boster, BM0135	WB (1:400)

mouse anti-E-cadherin	BD, 610182	WB (1:2000)
mouse anti-Snail	CST, 3895S	WB (1:800)
rabbit anti-Slug	Boster, PB0443	WB (1:400)
		WB (1:800)
rabbit anti-Twist I	CST,46702S	WB (1:800);
	Proteintech, 66828-1	IF/IHF (1:100)
mouse anti-VEGFA	CST, 2478S	WB/ICW
rabbit anti-phospho-		(1:800)
VEGFR2	Proteintech,67407-1	WB/ICW
rabbit anti-VEGFR2	Proteintech, 27309-1	(1:500)
rabbit anti-Ki67	CST, 9520S	WB (1:800); IF
rabbit anti-phospho-Smad3		(1:100)
rabbit anti-Smad3	CST, 9523S	WB (1:800)
rabbit anti-phospho-ERK-	CST, 9106S	WB (1:800)
1/2		WB (1:800)
rabbit anti- ERK-1/2	CST, 9102S	WB (1:800)
rabbit anti-phospho-AKT	CST, 4060S	WB (1:800)
rabbit anti-AKT		
	CST, 9272S	WB (1:800)
rabbit anti-p38	CST, 9212S	WB (1:800)
rabbit anti-phospho-p38	CST, 9211S	WB (1:800)
rabbit anti-GAPDH	Bioworld, AP0063	WB (1:8000)

mouse anti- α -Tubulin	Proteintech, 66031-1	WB (1:2000)
rabbit anti-CD31	Abcam, ab24590	IF (1:100)
rabbit anti-CD34	Abcam, ab81289	IF/IHF (1:100)
rabbit anti-CD9	Bioss, bs-2489R	WB (1:500)
rabbit anti-CD63	Abcam, ab134045	WB (1:1000)
rabbit anti-CD81	Bioss, bs-6934R	WB (1:500)
goat anti-rabbit IgG-HRP	CST, 7074	WB (1:4000)
horse anti-mouse IgG-HRP	CST, 7076	WB (1:4000)
goat anti-mouse-Alexa Fluor 488	Invitrogen A-11001	IF (1:500)
goat anti-mouse-Alexa Fluor Plus 555	Invitrogen A-21422	IF (1:500)
goat anti-mouse-Alexa Fluor Plus 633	Invitrogen A-21052	IF (1:500)
donkey anti-rabbit- Alexa Fluor Plus 555	Invitrogen A-31572	IF/IHF (1:500)
goat anti-mouse Alexa Fluor Plus 680	Invitrogen A-21057	IHF/ICW (1:500)
goat anti-rabbit Alexa Fluor Plus 790	Invitrogen A-11369	IHF/ICW (1:500)
rabbit-anti-LBH-FTIC	Lifespan LS-C672608	NFC (1:25)

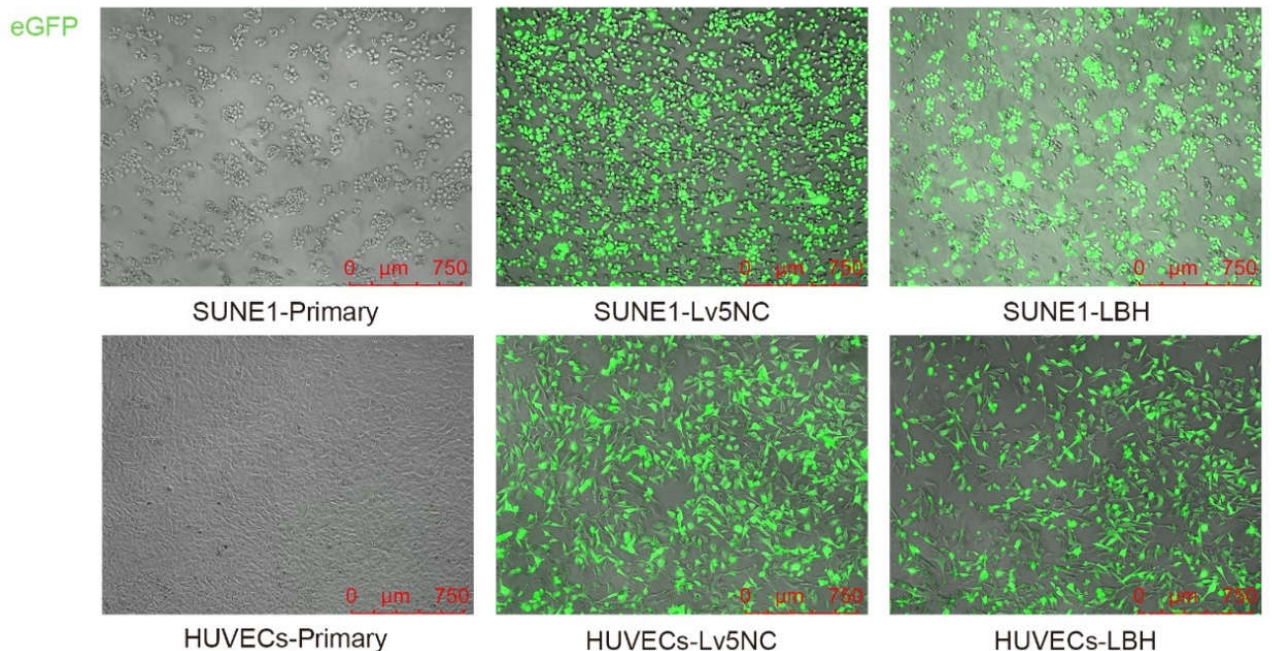
WB, Western blotting; IF, Immunofluorescence; IHF, Immunohistochemistry; ICW, In cell western; NFC, Nano-flow cytometry.

Supplemental Figure 1



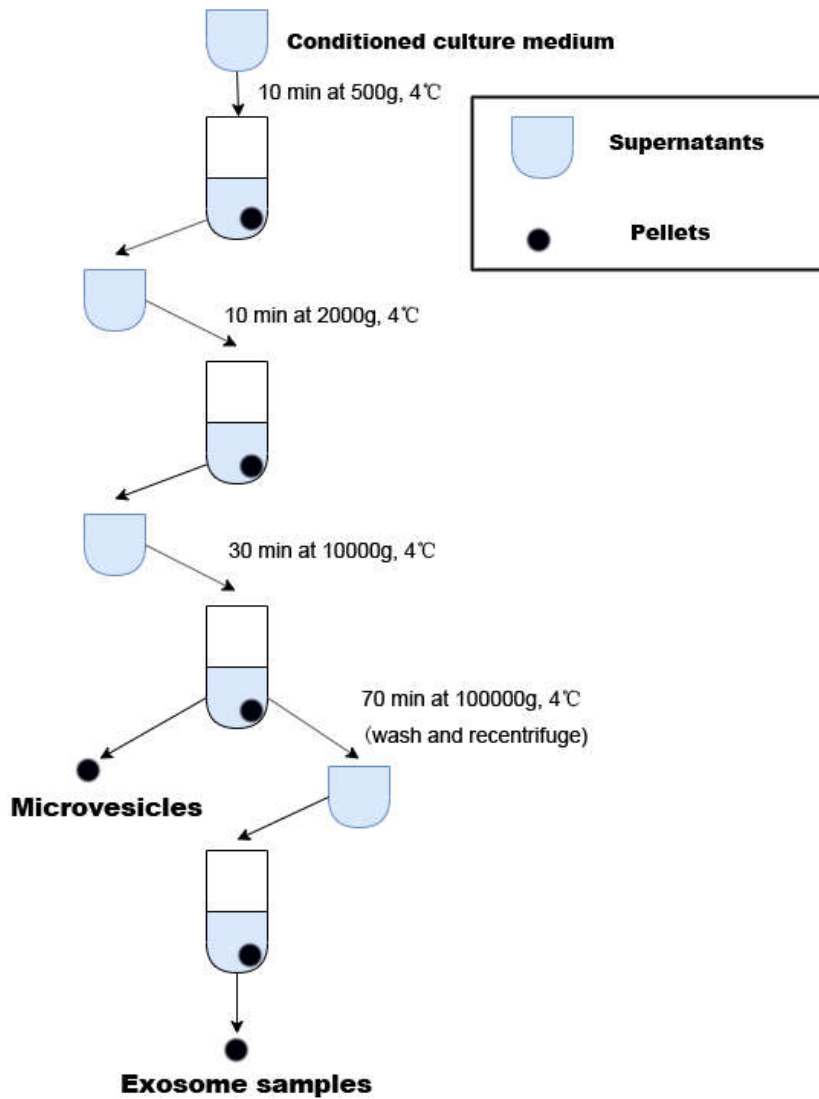
Supplemental Fig. 1 Representative immunofluorescence images of HUVECs for the staining of CD31 and CD34. The fact that the majority of tested cells were CD31⁺ and CD34⁺ verified the purity of HUVECs.

Supplemental Figure 2



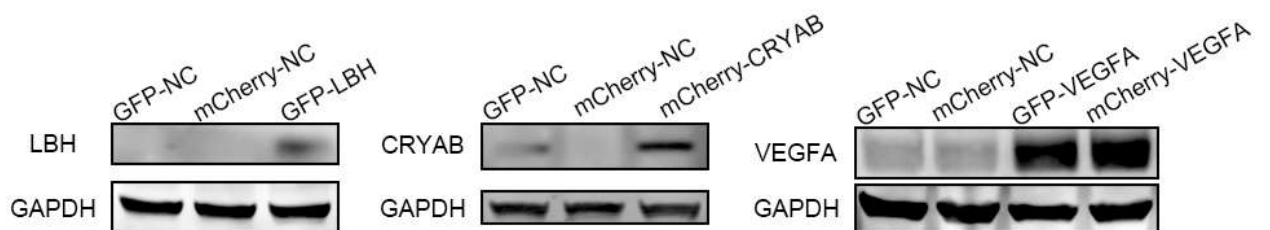
Supplemental Fig. 2 Fluorescence images indicating the infection efficiencies of SUNE1 and HUVECs cell lines prepared for the following experiments. The green fluorescence is expressed eGFP which was constructed in Lentivirus vectors.

Supplemental Figure 3



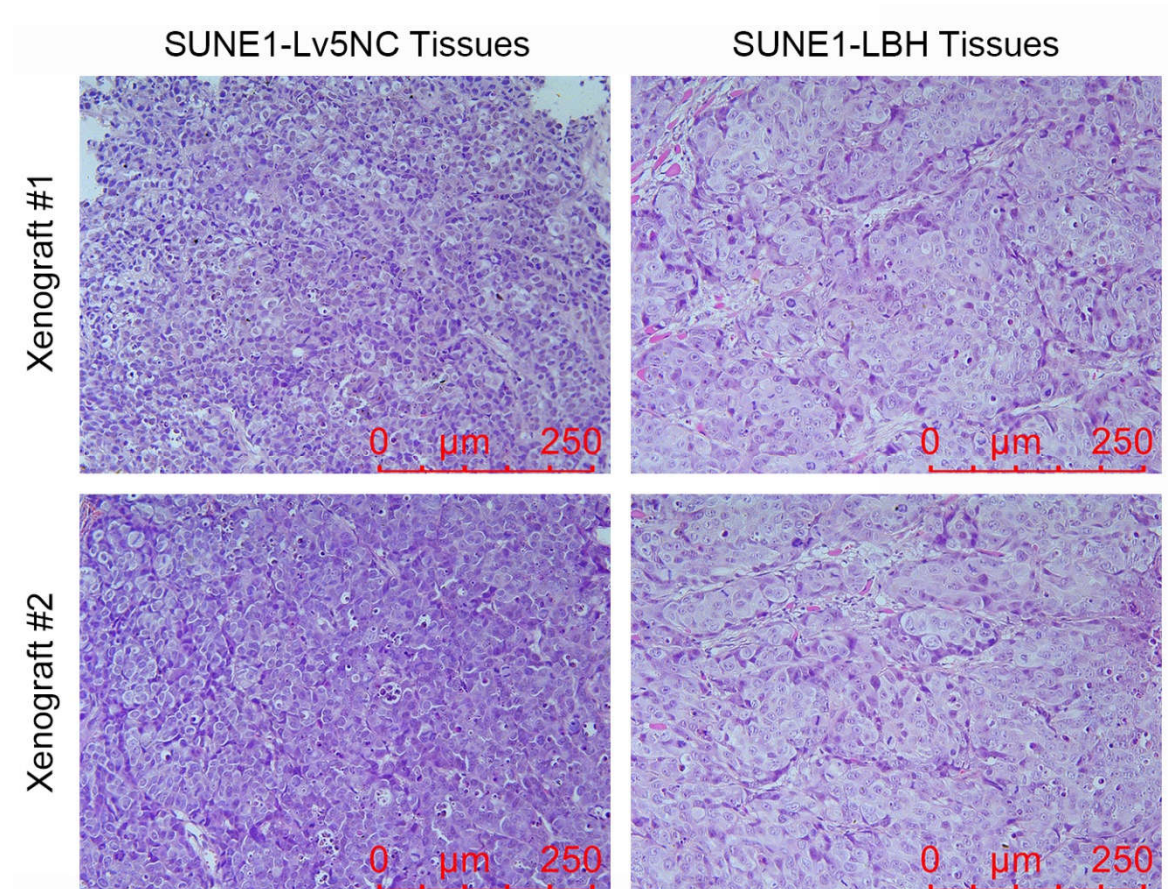
Supplemental Fig. 3 Protocols of exosome isolation by differential ultracentrifugation used in this study, presented as flowchart.

Supplemental Figure 4



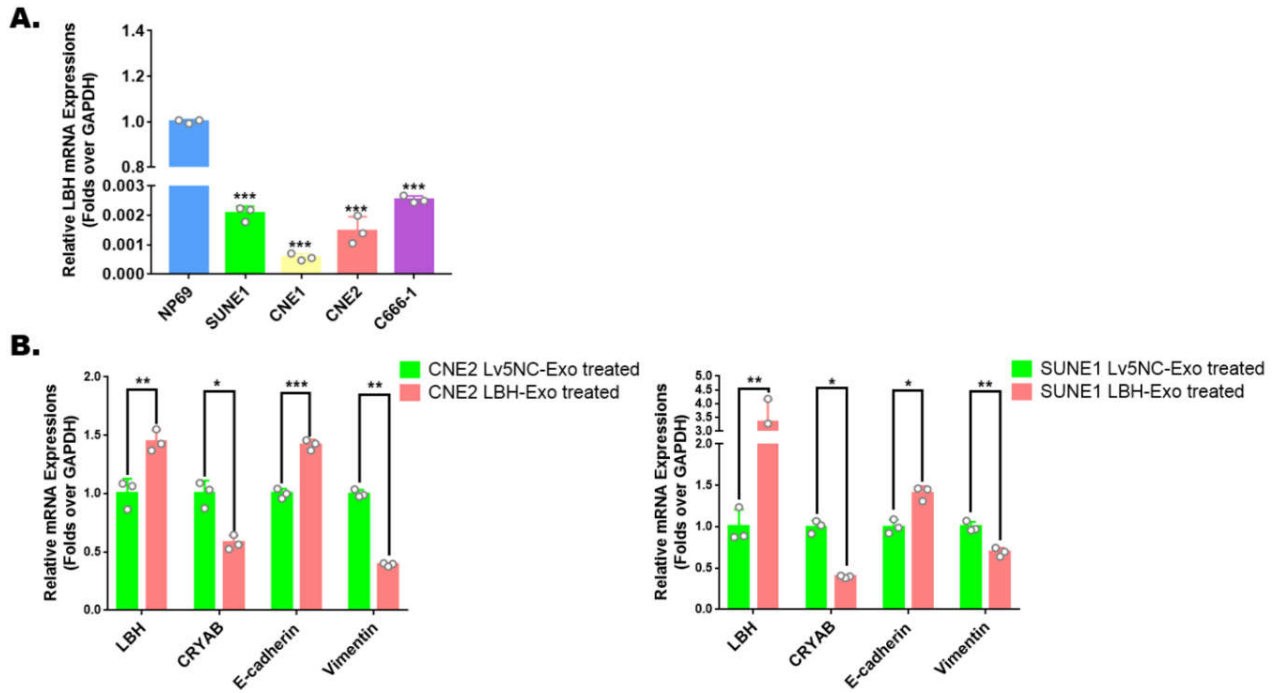
Supplemental Fig. 4 Representative image of Western blotting performed to validate the exogenous expressions of designated genes initiated by transfecting reconstructed plasmids into HUVECs. It confirmed the functions of reconstructed plasmids used for FRET assays in **Fig.7B**.

Supplemental Figure 5



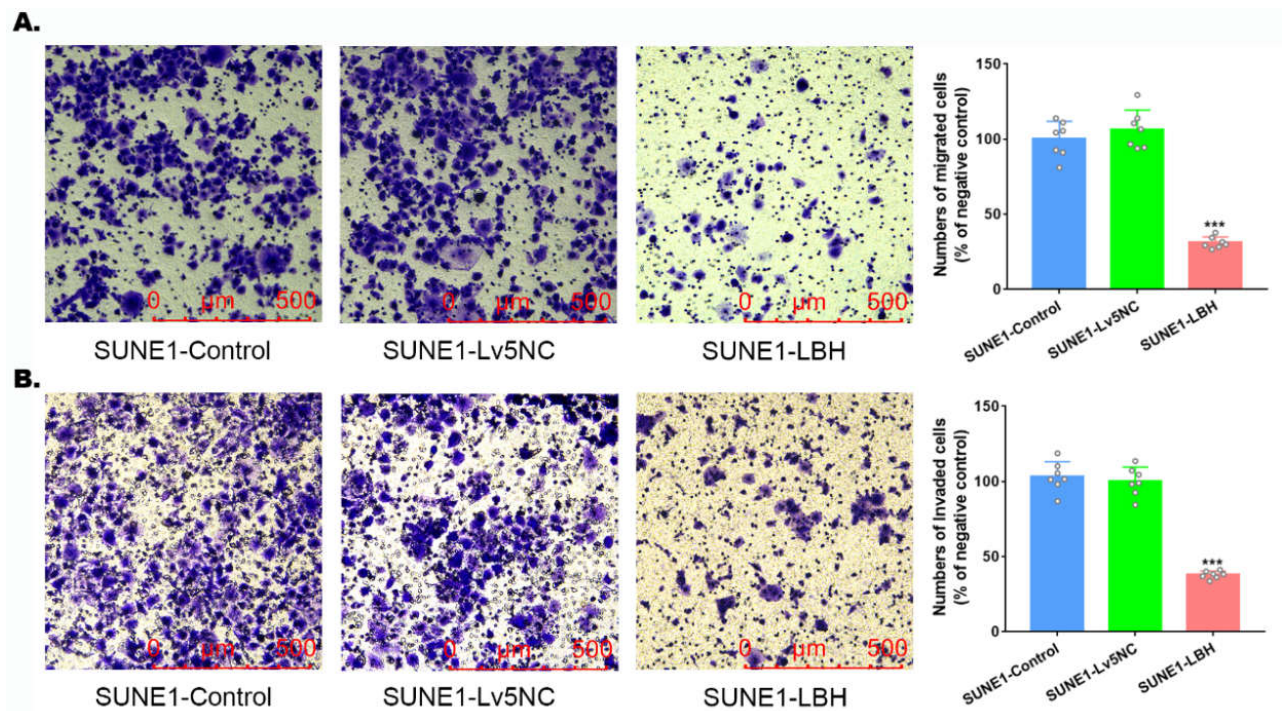
Supplemental Fig. 5 H&E staining of tumor xenografts constructed by LBH-overexpressed NPC cells. For SUNE1 NPC xenografts, the tissues of LBH-overexpressed tumors are well differentiated compared to the controls, which exhibited epithelial characteristics, while the tissues of Lv5NC tumors exhibited poorly differentiated, mesenchymal characteristics.

Supplemental Figure 6



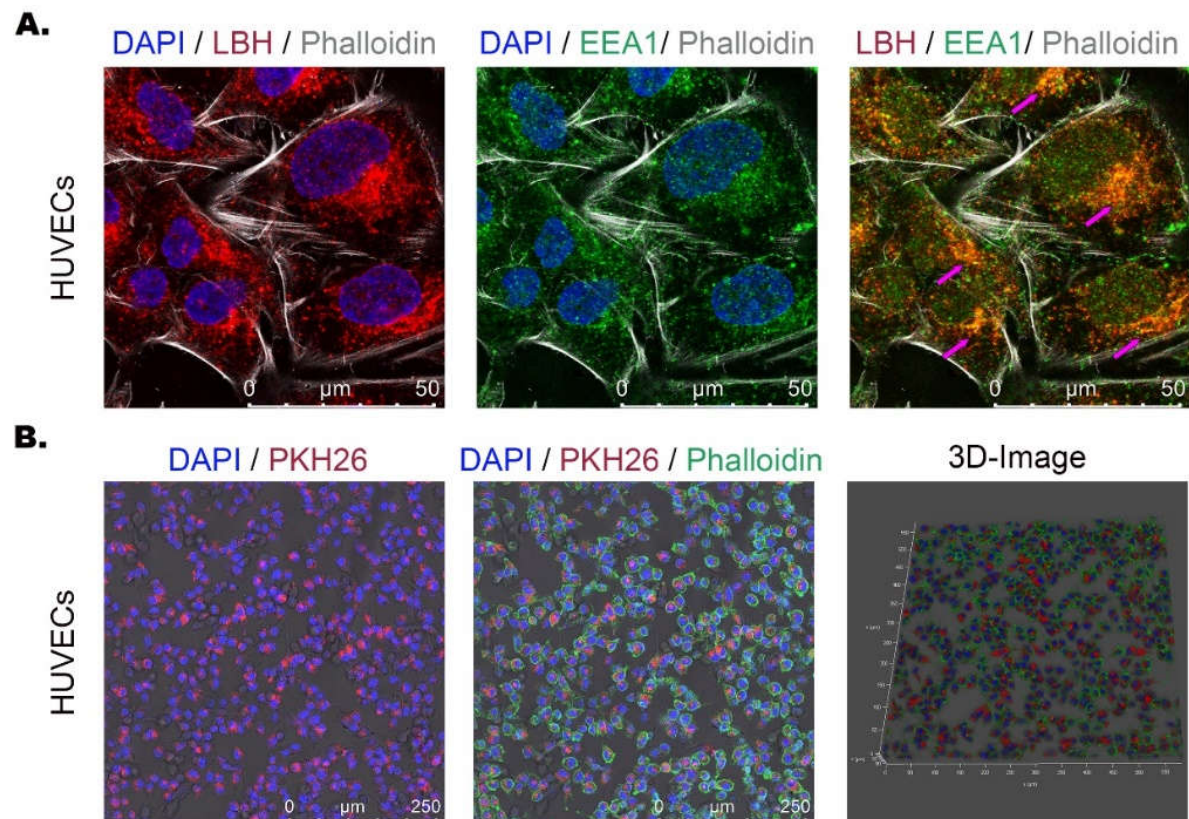
Supplemental Fig. 6 (A) mRNA levels of LBH in NP69 and NPC cell lines (** $p < 0.01$ and *** $p < 0.001$ vs. NP69). **(B)** mRNA levels of LBH, CRYAB, E-cadherin and Vimentin in NPC cells treated by NPC exosomes (* $p < 0.05$, ** $p < 0.01$ and *** $p < 0.001$ vs. Lv5NC-Exo treated).

Supplemental Figure 7



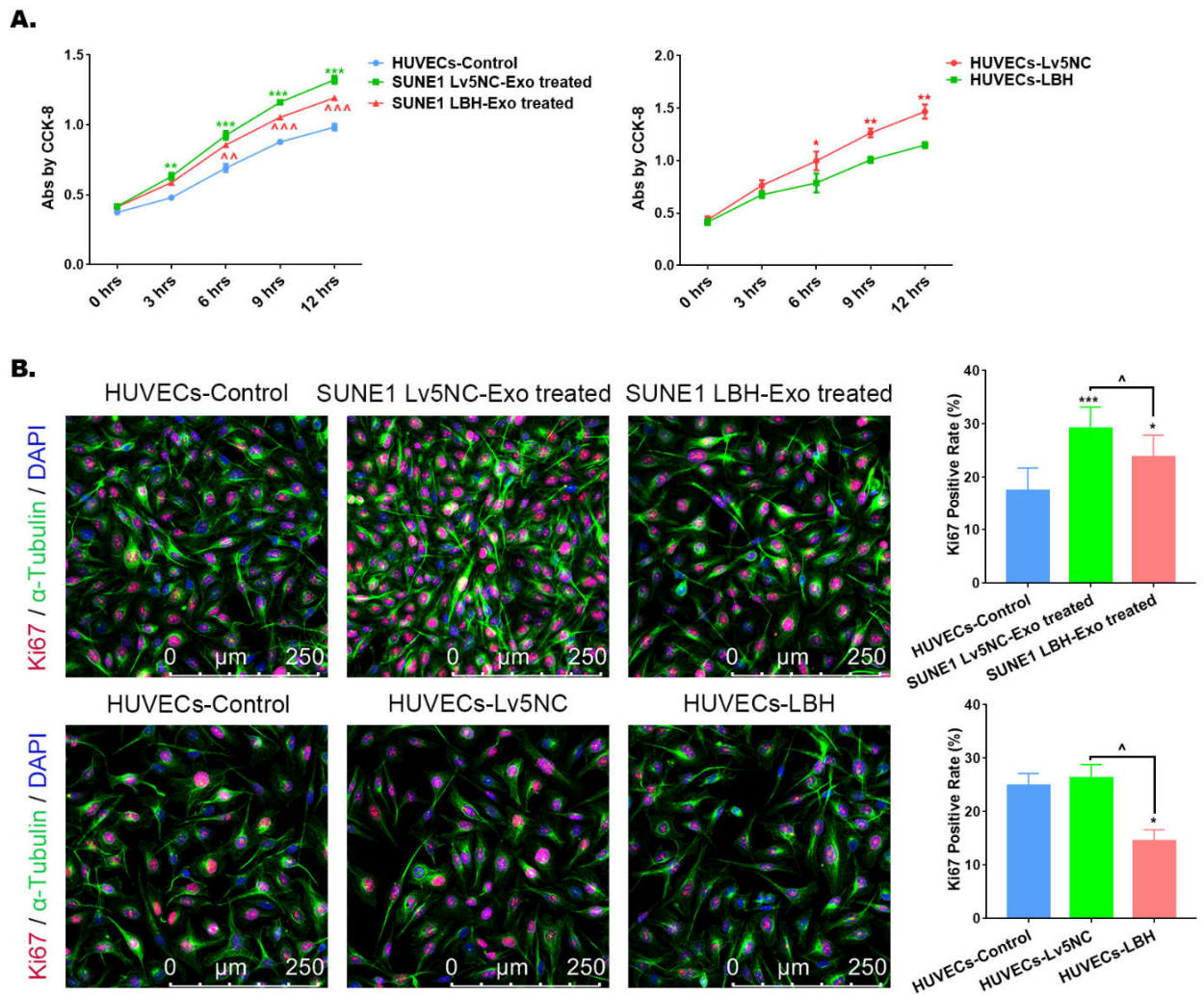
Supplemental Fig. 7 Representative images of the Transwell assay (A) and Matrigel Transwell assay (B) of SUNE1-Control, SUNE1-Lv5NC and SUNE1-LBH, and corresponding statistical analyses (***p*<0.001 vs. Control).

Supplemental Figure 8



Supplemental Fig. 8 (A) Representative confocal microscopic images of dual staining of anti-LBH (red) and anti-EEA1 (green) in HUVECs. Colocalization of LBH and EEA1 were observed in the perinuclear cytoplasm of HUVECs (Indicated by magenta arrows). **(B)** Representative confocal microscopic images of HUVECs treated by PKH26 labelled exosomes derived from SUNE1 cells. Both the 2D fluorescence images and the 3D reconstructed image confirmed the intracellular distribution of PKH26 labelled exosomes inside HUVECs, and some cells in the DAPI/PKH26/Phalloidin channel showed ongoing membrane fusion, which was indicated by merged signal of PKH26 and Phalloidin.

Supplemental Figure 9

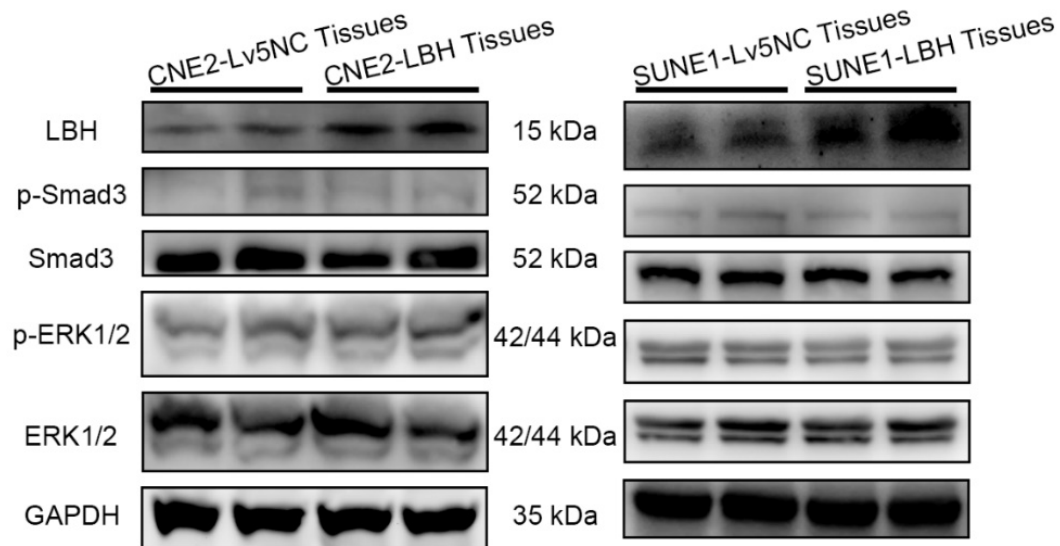


Supplemental Fig. 9 Cellular proliferation for HUVECs infected with LBH-overexpressed lentivirus or treated with NPC exosomes from LBH-overexpressed SUNE1 cells. Both the CCK-8 data and immuno-staining of Ki67 are in agreement with its proliferation of the same samples detected by EdU staining in **Fig. 5A**.

Supplemental Figure 10

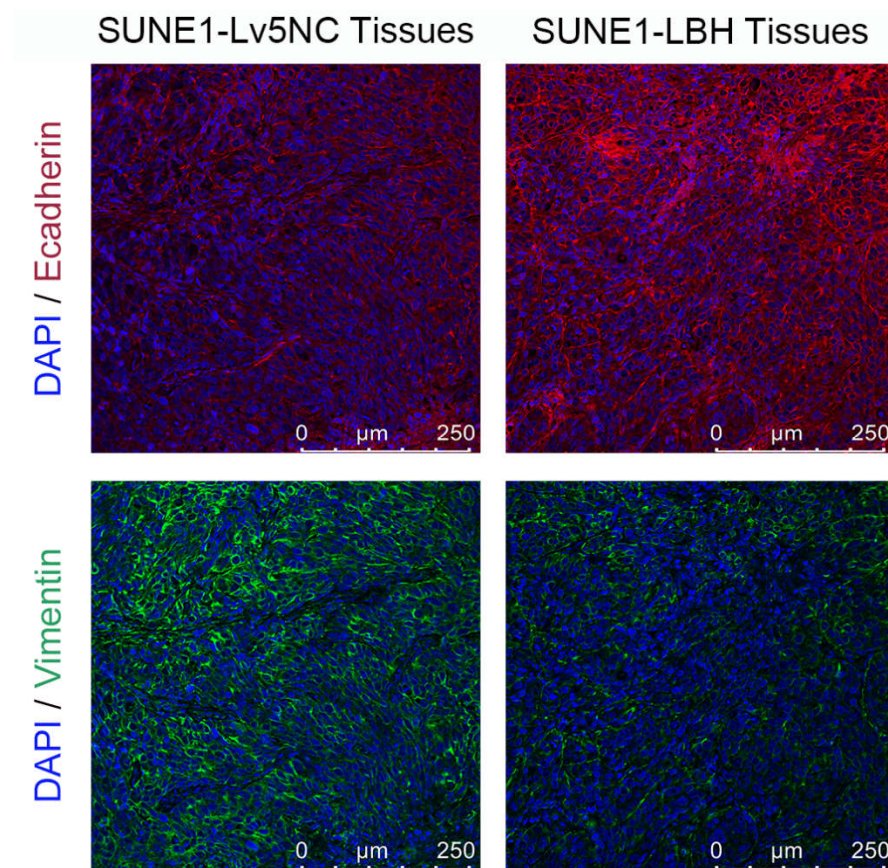
upregulation confirmed that the function of LBH to inhibit VEGFA signaling is modulated by downregulating CRYAB in HUVECs.

Supplemental Figure 12



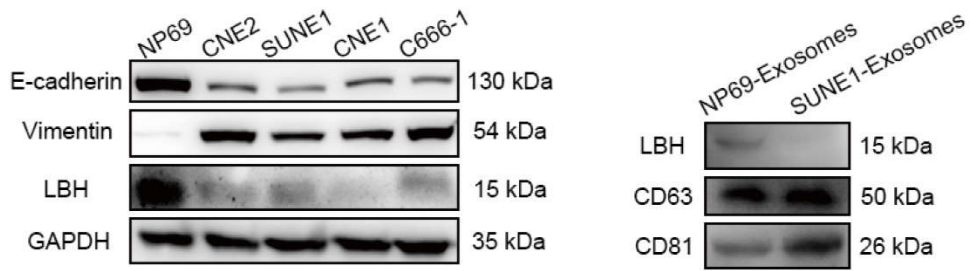
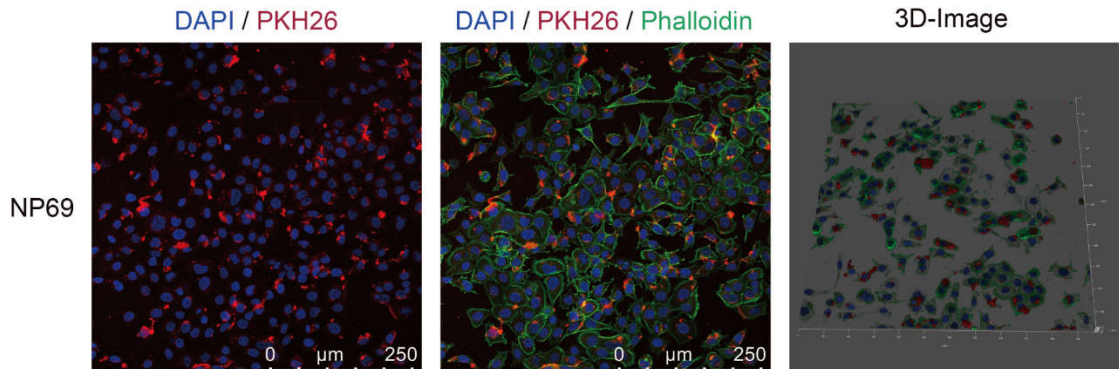
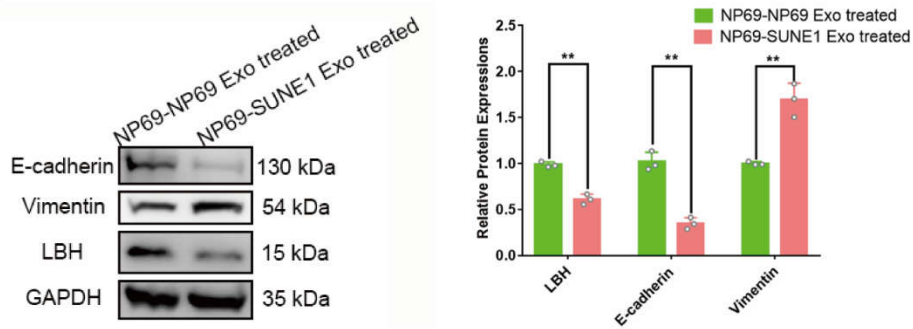
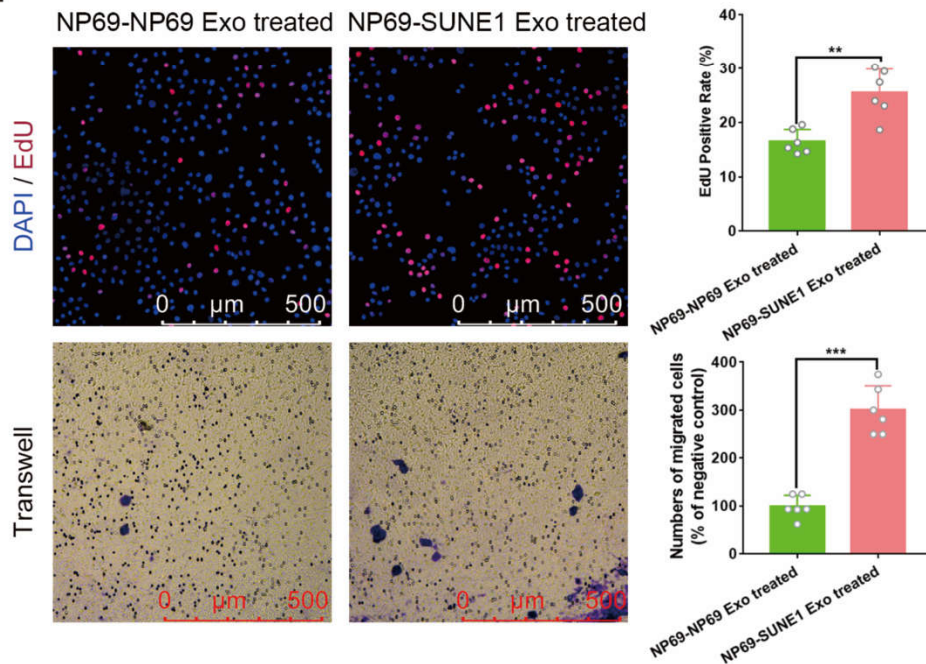
Supplemental Fig. 12 Part of downstream cascades in VEGFA/VEGFR2 signaling in NPC xenograft tumor tissues that was not affected by LBH-overexpression. The WB results of the parallel cascades of VEGFA/VEGFR2 signaling, namely AKT and P38 pathways were showed in **Fig. 8B**.

Supplemental Figure 13



Supplemental Fig. 13 EMT progressions of tumor xenografts constructed by LBH-overexpressed NPC cells were indicated by co-staining of anti-E-cadherin and anti-Vimentin. For SUNE1 NPC xenografts, the tissues of LBH-overexpressed tumors exhibited upregulated epithelial marker E-cadherin, as well as downregulated mesenchymal marker Vimentin compared to the tissues of Lv5NC tumors, which implied that LBH overexpression is correlated with inhibited EMT of NPC tumor xenografts.

Supplemental Figure 14

A.**B.****C.****D.**

Supplemental Fig. 14 The effects of LBH+ NPC exosomes on nasopharyngeal epithelial cell line NP69. **(A)** Western blotting verified elevated LBH expression and epithelial characteristics in NP69 cells compared to multiple NPC cell lines; NP69-derived exosomes showed higher LBH protein level compared to NPC-derived exosomes. **(B)** Representative confocal microscopic images of NP69 treated by PKH26 labelled exosomes derived from SUNE1 cells. Both the 2D fluorescence images and the 3D reconstructed image confirmed the intracellular distribution of PKH26 labelled exosomes inside NP69 cells. **(C)** Protein levels of LBH, Vimentin and E-cadherin in NP69 cells treated with NP69-derived exosomes or SUNE1-derived exosomes (**p<0.01 vs. Lv5NC-Exo treated). **(D)** Representative images of the Transwell assay and EdU assay of NP69 cells treated with NP69-derived exosomes or SUNE1-derived exosomes, and corresponding statistical analysis (**p<0.01 and ***p<0.001 vs. Lv5NC-Exo treated).